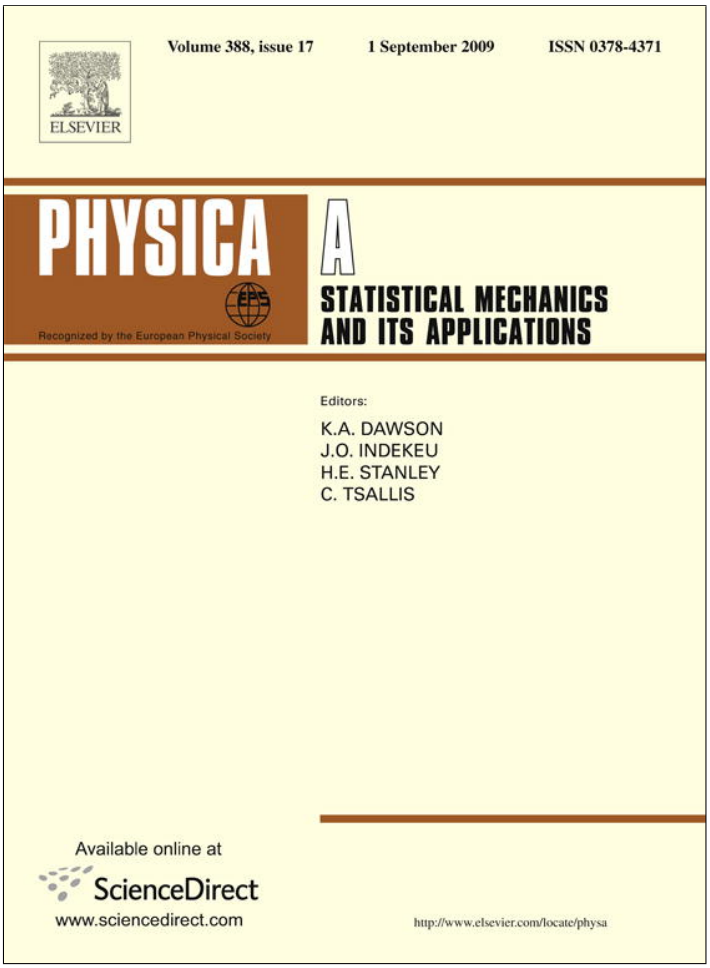

Physica A 388 (2009) 3600–3608

Contents lists available at ScienceDirect

Physica A

journal homepage: www.elsevier.com/locate/physa

A modification of the Social Force Model can reproduce experimental data of pedestrian flows in normal conditions

Daniel R. Parisi [a,b,*], Marcelo Gilman [a], Herman Moldovan [a]

[a] URBIX TECHNOLOGIES Research Division, Céspedes 2685, 6°A, C1426DUK, Ciudad Autónoma de Buenos Aires, Argentina

[b] CONSEJO NACIONAL DE INVESTIGACIONES CIENTÍFICAS Y TÉCNICAS, Av.Rivadavia 1917, C1033AAJ, Ciudad Autónoma de Buenos Aires, Argentina

ARTICLE INFO

Article history:
Received 22 October 2008
Received in revised form 14 May 2009
Available online 27 May 2009

PACS:
45.70.Vn
89.65.-s
89.65.Lm
05.90.+m

Keywords:
Pedestrian dynamics simulation
Social force model
Specific flow rate
Fundamental diagram

ABSTRACT

The Social Force Model presents some limitations when describing the experimental data of pedestrian flows in normal conditions — in particular the specific flow rates for different door widths and the fundamental diagram.

In the present work we propose a modification of this model that consists of a self-stopping mechanism to prevent a simulated pedestrian from continuously pushing over other pedestrians.

With this simple change, the modified model is able to reproduce the specific flow rates and fundamental diagram of pedestrian flows for normal conditions, as reported in the literature.

1. Introduction

1.1. Pedestrian dynamics characterization

Pedestrian dynamics exhibit, in a first approximation, two distinct behavioral states:

- Normal (cooperative, no pushing, stop before enter in physical contact)
- Competitive or Panic (pushing, with disregard for contacting or hurting other people)

While the competitive state is difficult to characterize empirically under controlled conditions (due to the risk of hurting people), the normal behavior of a crowd can be studied via macroscopic measurement. In this work, we will focus on the normal state.

In this state, the main macroscopic observables that characterize pedestrian dynamics are: (a) the *specific flow rate* (number of persons crossing an opening per unit of time and width) and (b) the *fundamental diagram* that indicates the relationship between local density and velocity.

Most legal regulations accept that the *specific flow rate* (p/m/s) exhibited by a system of evacuating people in normal conditions remains constant if the door width changes. Some regulations adopt a specific flow rate of around 1.33 p/m/s (see Table 1).

* Corresponding author at: URBIX TECHNOLOGIES Research Division, Céspedes 2685, 6°A, C1426DUK, Ciudad Autónoma de Buenos Aires, Argentina. Tel.: +54 911 6707 8805; fax: +54 11 4785 0185.

E-mail addresses: dparisi@urbix.com.ar (D.R. Parisi), mgilman@urbix.com.ar (M. Gilman), hmoldovan@urbix.com.ar (H. Moldovan).

0378-4371/$ – see front matter © 2009 Elsevier B.V. All rights reserved.
doi:10.1016/j.physa.2009.05.027

Table 1
Some mean and design values of specific flow rate reported in the literature.

Specific flow rate (p/m/s)	Bibliographic source
1.33	[1]
1.37	[2]
1.82	[3]
1.48–1.92	[4]
1.25–1.4	[5]
1.77	[6]
1.33	[7]
1.9	[8]
1.97	[9]

However, experimental results from the literature report different values for this magnitude, ranging from 1.25 to 2.0 p/m/s, as shown in Table 1, depending on the particular set-up conditions, age and perhaps culture of the population. In hurry situations, specific flow rates greater than 4 p/m/s were observed.

Regarding the fundamental diagram (i.e. mean velocity versus local density plot) there exist a variety of experimental data reported in the literature [9–19] considering experiments and field observations in different situations and cultures.

There are some differences between these fundamental diagrams; nevertheless all of them show a monotonically decreasing velocity as the density increases.

1.2. Pedestrian dynamics modeling

Although many mathematical models (continuous and cellular automata) have been developed in the last decades, validation of macroscopic observables with empirical data is seldom found.

As a conceptual frame for modeling pedestrian movements, we will refer to the hierarchical view introduced by Hoogendoorn [20] that assumes that there are different levels of complexity involved in pedestrian navigation: Operational (basic walking behavior), Tactical (server selection, route choice) and Strategical (general planning).

Our goal is to find a model, simple enough to be limited to the Operational level, but that can reproduce the main observables of pedestrian dynamics in normal conditions.

The Social Force Model (SFM) of Helbing, et al. [21,22] is a famous continuous model for describing pedestrian dynamics that qualitatively reproduces many self-organizing phenomena like lane formation, clogging or "faster is slower". This model may be appropriate for describing the low level mechanism of navigation (Operational level), if it is able to reproduce the basic physical movements and the main physical macroscopic observables for many persons in relatively simple geometries.

We propose that more complex mechanisms like realistic (moving or fixed) obstacle avoidance, wayfinding and decision making should be resolved in higher levels of modeling (Tactical and Strategical levels).

The SFM, as formulated in Ref. [22], states that the dynamics of N_p pedestrians (particles) is governed by three forces: the Desire Force (self-propulsion of the particles), the Social Force (repulsive interaction with infinite range) and the Granular Force (physical contact interactions). A primary parameter of the SFM is the desired velocity, v_d, that is related to the propulsive force of each particle.

In the paper [22], the parameters of the model were chosen in order to reproduce the flow through bottlenecks measured in Ref. [10]. Specifically, it reproduces the specific flow rate of 0.73 p/m/s for a 1 m door width and desired velocity $v_d = 0.8$ m/s.

For our implementation (presented in Sections 3.1 and 3.2) with desired velocities corresponding to pedestrians in normal conditions, neither the values of a constant specific flow rate at exits of different widths, nor the observed relationship between pedestrian density and velocity can be reproduced, as will be shown in Section 3.

The explanation for this is that the Social Force Model is a competitive model for all values of the desire velocities.

At first view, the desired velocity, v_d, can be interpreted as a parameter that allows tuning between cooperative and competitive behavior. This concept is not totally true. Indeed, this parameter indicates the movement capacity of the pedestrian, which is not necessarily related to a particular degree of competitiveness or hurry.

During an egress process, a high v_d may be interpreted as a high level of competitiveness. However, a pedestrian moving with a low v_d does not indicate cooperative behavior necessarily, because this low velocity may be the maximum velocity attainable for this pedestrian.

Consider, for example, an aged person or a little child or a handicapped person trying to flee from a danger. His/her velocity may be low, but this does not mean that he/she is not in panic.

This counterexample is sufficient to demonstrate that a pedestrian with a low v_d does not implies always a cooperative behavior.

Furthermore, in spite of this lower velocity, the pedestrian must be considered in a competitive state if he/she does not stop pushing other pedestrians interfering in his/her way. A pedestrian in a normal state would try to stop before making physical contact.

Pedestrians in the SFM model lack of any self-slowing mechanism. Therefore they always push with disregard of contacting other simulated people. Consequently, by definition of competitive behavior, it can be asseverated that this model describes competitive pedestrians for all v_d.

It must be noted that for low v_d, the social force can prevent contact. But the absence of contact does not implies the absence of push, which is exerted via the social force.

There are several other implementations of the SFM [21,23–26], with variations in the social force term. None of these implementations includes a self-stopping mechanism. Furthermore, it is known that the qualitative phenomena described by this model do not change when the functional form of the social repulsive term changes [26].

Thus, if this model is intended to be used in the description of pedestrian flows in normal conditions, it must modified to account for some self-slowing, as highlighted above. It is natural to include a new mechanism into the model that allows simulated pedestrians to decelerate under certain situations.

1.3. Other modifications to the Social Force Model

Previous works have made important contributions to improve different aspects of the SFM:

- Lakoba et al. [27] have proposed modifications to include realistic parameters in the SFM, eliminate non-realistic behavior for few simulated pedestrians and, at the same time, conserve its ability to simulate observed behavior for systems with a large number of pedestrians.
  They modified the SFM with several new mechanisms (e.g. memory effects and density effects) in the social repulsion force.
  The complexity of these mechanisms corresponds to higher levels of modeling. The ideal way to include them would be through new models for the Tactical and Strategical layer. This would allow maintaining a simple model for the lowest (Operational) level.
- Seyfried et al. [15,19] have made an important contribution by studying the 1-D fundamental diagram (a single line of persons in a close loop). The authors conducted experiments and proposed a modification to the SFM that can reproduce the experimental data.
  Their modifications differ from the one proposed in the present work, and they will be discussed in Section 2.

1.4. Organization of the paper

The present work is organized as follows: In Section 2 the Modified Social Force Model is presented. Section 3 shows the results of the introduced model when simulating two systems: (a) the egress from a square room and (b) a circular racetrack. The specific flow rate for different door widths and the fundamental diagram are calculated. Comparison between the original and modified model is shown. Finally in Section 4 the conclusions are presented.

2. The modified Social Force Model

In the Social Force Model proposed by Helbing et al. [22], the dynamics of each pedestrian (p_i) are driven by three forces with different properties. They are the Desire Force, $\mathbf{F}_{Di}$, the Social Force, $\mathbf{F}_{Si}$, and the Granular Force, $\mathbf{F}_{Gi}$. The corresponding expressions are:

$$\mathbf{F}_{Di} = m_i \frac{(v_{di}\mathbf{e}_i - \mathbf{v}_i)}{\tau_i} \tag{1}$$

where m_i is the particle mass, $\mathbf{v}_i$ is the actual velocity, v_{di} is the magnitude of desired velocity, $\mathbf{e}_i$ is the unit vector pointing to the desired target, and τ_i is a time constant related to the relaxation time of the particle to achieve v_{di}.

$$\mathbf{F}_{Si} = \sum_{j=1, j\neq i}^{N_p} A \exp\left(\frac{-\varepsilon_{ij}}{B}\right) \mathbf{e}_{ij}^n \tag{2}$$

where N_p is total number of pedestrians in the system, A and B are constants that determine the strength and range of the social interaction, $\mathbf{e}_{ij}^n$ is the unit vector pointing from particle p_j to p_i, i.e. the normal direction between two particles, and

$$\varepsilon_{ij} = r_{ij} - \left(R_i + R_j\right) \tag{3}$$

where r_{ij} is the distance between the centers of p_i and p_j, and R is the particle radius.

$$\mathbf{F}_{Gi} = \sum_{j=1, j\neq i}^{N_p} \left[\left(-\varepsilon_{ij} k_n\right) \mathbf{e}_{ij}^n + \left(v_{ij}^t \varepsilon_{ij} k_t\right) \mathbf{e}_{ij}^t\right] g(\varepsilon_{ij}). \tag{4}$$

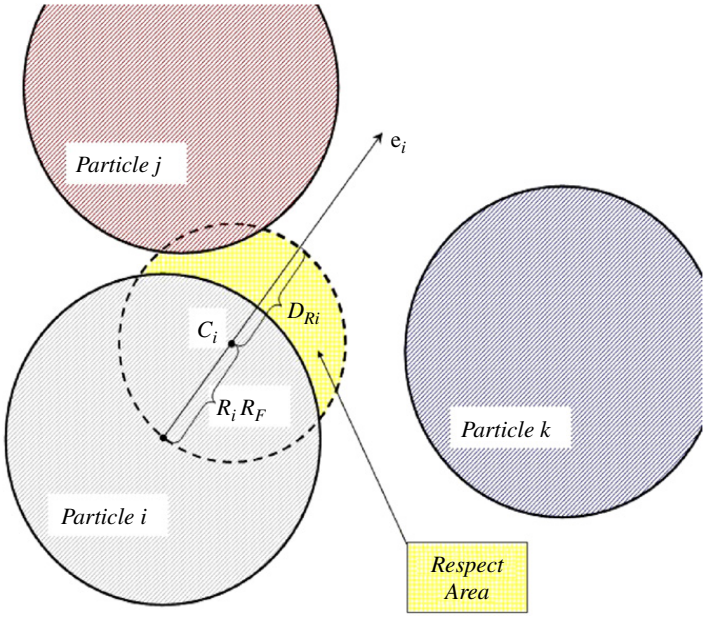

Fig. 1. Geometry of the Respect Area for the particle *i*. Particle *j* is inside the respect area of particle *i* and particle *k* is not. While the area is entered, the respect mechanism sets $v_{di} = 0$.

Here the tangential unit vector $\mathbf{e}_{ij}^t$ indicates the perpendicular direction to $\mathbf{e}_{ij}^n$, $k_n$and k_t are the normal and tangential elastic restorative constants, v_{ij}^n is the normal projection of the relative velocity seen from $p_j(\mathbf{v}_{ij} = \mathbf{v}_i - \mathbf{v}_j)$, v_{ij}^t is the tangential projection of the relative velocity, and the function $g(\varepsilon_{ij})$ is 1 if $\varepsilon_{ij} < 0$ and 0 otherwise.

The interaction of particles with walls and corners is computed using the social and granular forces in an analogous way.

As it will be shown in Sections 3.1 and 3.2, the SFM is not able to reproduce experimental data of pedestrians in normal conditions. Therefore a "respect" mechanism is introduced.

Let us define the *respect factor*, R_F, to be a positive real number. The *respect distance*, D_R for the particle *i* is the product of the respect factor times its radius:

$$D_{Ri} = R_F R_i. \tag{5}$$

Now consider a point C_i that lies on the direction of $\mathbf{e}_i$ (the direction of the desired velocity) and is located at a distance D_{Ri} from the center of the particle *i*.

The *respect area* for pedestrian *i* is given by the circle with center at C_i and radius D_{Ri} as shown in Fig. 1.

If any other particle touches the respect area (as particle *j* does in Fig. 1), the magnitude of the desired velocity of particle *i*, v_{di}, is set to 0 until the respect area is free again. Only then does pedestrian *i* recover $v_{di} > 0$ and so become self-propelled again.

The step functional form was chosen because it is the simplest self-stopping mechanism that reproduces the known experimental data, as shown in the next section.

In a real system, this self-stopping mechanism represents a last resource action when, due to the failure of higher-level avoidance mechanisms, another pedestrian gets too close.

When the respect area is entered, only $v_{di}$is set to 0. The model states that the instantaneous velocity v_i, continues to be integrated normally, allowing the particle *i* to continue its movement (v_i may be non-zero). Artificial stops do not occur for particles that are close in cases of low densities or in face-to-face encounters. Indeed, the proposed modified model is able to reproduce "lane formation" for counter flow in a narrow corridor.

It must be noted that the respect mechanism belongs to the microscopic domain, in the sense that it is a basic rule acting at the agent level, from which emerges a collective behavior of the crowd. Furthermore, this rule does not have any information about the macroscopic observables that the model is expected to reproduce.

As stated in Section 1, a different modification to the SFM was proposed by Seyfried et al. [19] studying the fundamental diagram in a 1-D system [15]. The main differences with the present model, are:

(a) The social force term was different to Eq. (2).
(b) The "required length of a pedestrian to move", in some ways equivalent to the respect distance, D_R, was considered variable as a function of the velocity. This functionality was obtained via macroscopic measurements of real systems.
(c) When the slowing-down condition is reached, the velocity of the pedestrian is set to zero ($v_i = 0$). In our model, the magnitude of the instantaneous velocity can be non-zero ($v_i \neq 0$) while the magnitude of the desired velocity is set to zero ($v_{di} = 0$). This produces a continuous slowing down instead of a sudden stop.

3. Simulations

The model described in Section 2 was implemented in the pedestrian simulation platform developed by Urbix Technologies.

The system of N_p ordinary coupled differential equations determining the dynamics of the particles are solved using the Verlet Algorithm [28] with a fixed time step of 1e-4 s.

The time required to simulate one realization of the egress of 600 people is 4 h on a 1.80 GHz Intel Dual Core Processor.

3.1. Specific flow rate

To examine the specific flow rate exhibited by the modified model, simulations of pedestrians leaving a 20 m × 20 m square room with one exit were conducted. All the walls delimiting the room have no thickness, i.e. each wall is simulated only by one line.

The pedestrians' parameters mass, m, shoulder width, d, and desired velocity, v_d, were uniformly distributed within the following ranges:

$m \in [70\text{ kg}, 90\text{ kg}]$

$d \in [0.50\text{ m}, 0.58\text{ m}]$

$v_d \in [0.9\text{ m/s}, 1.5\text{ m/s}]$.

The social force model parameters used were:

$k_n = 1.2e5\text{ N/m}$;

$k_t = 2.4e5\text{ kg/m/s}$;

$A = 2e3\text{ N}$;

$B = 0.08\text{ m}$;

$\tau = 0.5\text{ s}$.

Particles inside the room have their targets located at the nearest position within the limits of the exit door.

The initial positions of pedestrians were uniformly distributed inside the room in such a way that $\varepsilon_{ij} > 0$ (i.e. pedestrians are not in contact) for all pairs ij. The initial velocities were set to zero for all particles.

Exit widths, L, of 1.2 m, 2.7 m and 3.2 m were considered, in the room containing 200, 500 and 600 pedestrians, respectively. Increasing door width with increasing number of pedestrians is used because in real systems, wider exits are required to evacuate more populated facilities. These values were chosen in accordance with the method of determining egress capacity stated in Chapter 7 of the "NFPA 101 *Life Safety Code* (2000 Edition)" that indicates a minimum capacity factor of 0.5 cm per person.

The respect factor, R_F, was varied to investigate its impact on the specific flow rate of the system. The values considered were $R_F = 0$; 0.25; 0.50; 0.75; 0.85 and 1.00.

The results of the simulations are shown in Fig. 2. The mean specific flow rate (measured as Total Number of pedestrians/Total Evacuation Time/L) is displayed as a function of R_F for the room studied with different door widths.

For low values of R_F the specific flow rate is not constant, but varies for the different door widths. The highest variations are observed for the case $R_F = 0$ (which corresponds to the original SFM).

The SFM shows that the wider the door is and – more importantly – the more populated the room is, the higher the specific flow rate. This effect is explained by two factors.

First, as discussed in Section 1, the SFM is a competitive model for all v_d, so pedestrians continually push via contact and/or social forces (because the social force is a force with infinite range).

Second, in the high density set of pedestrians near the door, their desire forces (Eq. (1)) became balanced by the social forces (Eq. (2)). These forces are propagated in a cumulative way through the crowd, producing a social force pressure near the door proportional to the number of pedestrians in the crowd inside the room.

To demonstrate the influence of the social pressure (generated by the number of pedestrian) in the specific flow rate, the following simulations were made considering the original SFM ($R_F = 0$):

(a) Changing the door width for fixed number of pedestrians ($N_p = 400$).
(b) Changing N_p for fixed door width ($L = 2.7$ m).

Fig. 3 shows the results.

It can be seen that the specific flow rate increases monotonically as the population (N_p) increases (Fig. 3(a)). On the other hand, if N_p is fixed, the increasing of the door width does not lead to any monotonic tendency of the specific flow rate (Fig. 3 (b)). From where it can be concluded that, for the original SFM, the increment in the number of pedestrians in the room is responsible for the increment in the specific flow rate.

Now, going back to Fig. 2, when increasing the value of R_F the curves for different door widths start to converge because the respect mechanism reduces the influence of social interaction by increasing the mean interpersonal distance.

Choosing $R_F \approx 0.7$ leads to a range of specific flow rates between 1.2 and 2 p/m/s, that correspond to egress under normal conditions, as listed in Table 1.

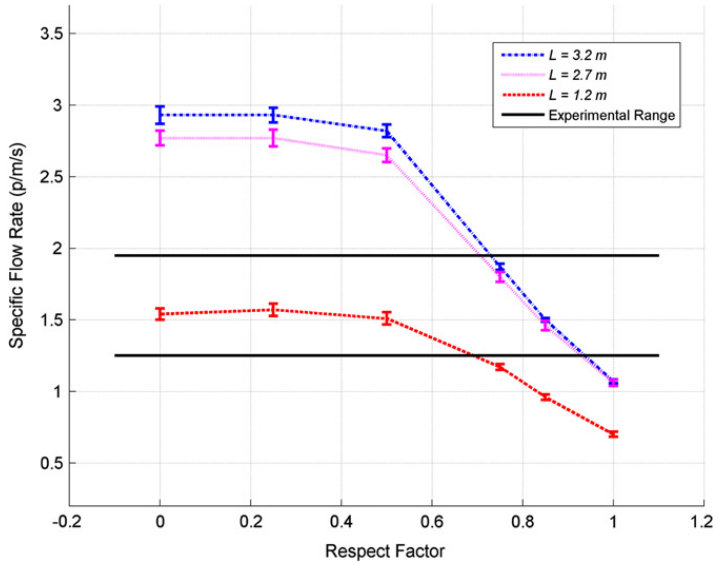

Fig. 2. Variation of the mean specific flow rate with the Respect Factor for different door sizes and number of occupants (1.2 m – 200 p; 2.7 m – 500 p and 3.2 m–600 p). Error bars indicate two standard deviations.

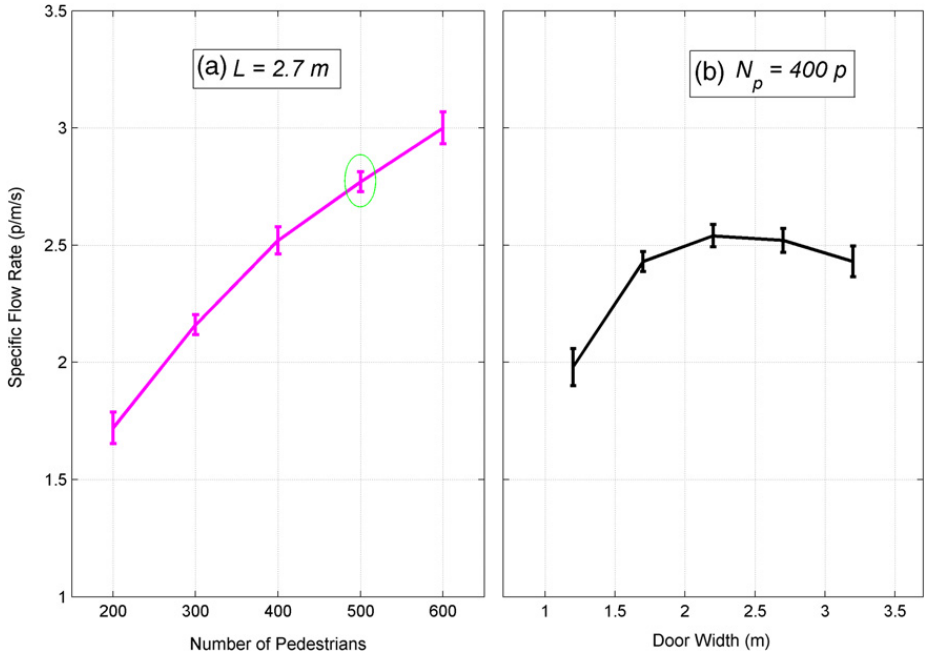

Fig. 3. (a) Variation of the mean specific flow rate with the number of pedestrians (N_p) leaving $L = 2.7$ m fixed; (b) Variation of the mean specific flow rate with the door width (L) leaving $N_p = 400$ p fixed. These curves were calculated with R_F=0. The point marked by a circle indicates the only point that is also present in Fig. 2.

3.2. Fundamental diagram

In this section, the ability of the proposed model to reproduce the observed fundamental diagram is studied.

The geometry of the simulated system is a racetrack, as shown in Fig. 4.

The pedestrians' characteristics and parameters were the same as in Section 3.1, except that the desired velocity, v_d, was uniformly distributed between 1.1 and 1.5 m/s.

Using the result obtained in Section 3.1 (see Fig. 2), the respect factor chosen for these simulations was $R_F = 0.7$.

The number of pedestrians in the racetrack circuit was varied to study the dynamics for different densities. Simulations with $N_p = 5$; 20; 80; 140; 200; 260; 320; 380 and 400 pedestrians were performed.

Pedestrians were initialized outside the racetrack in an adjacent corridor designated in Fig. 4 as "Pedestrian Access". The density in the corridor was set similarly to the final density in the racetrack.

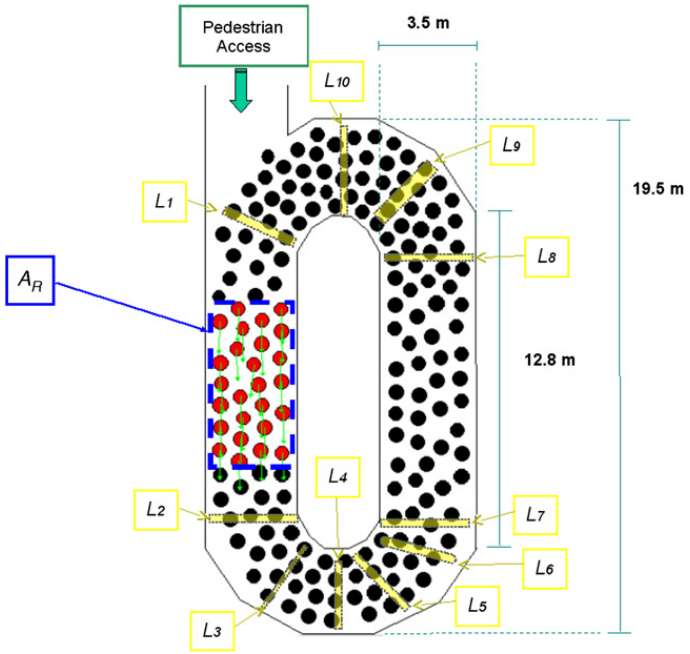

Fig. 4. Geometry of the simulated system for the measurement of the fundamental diagram with around 200 pedestrians.

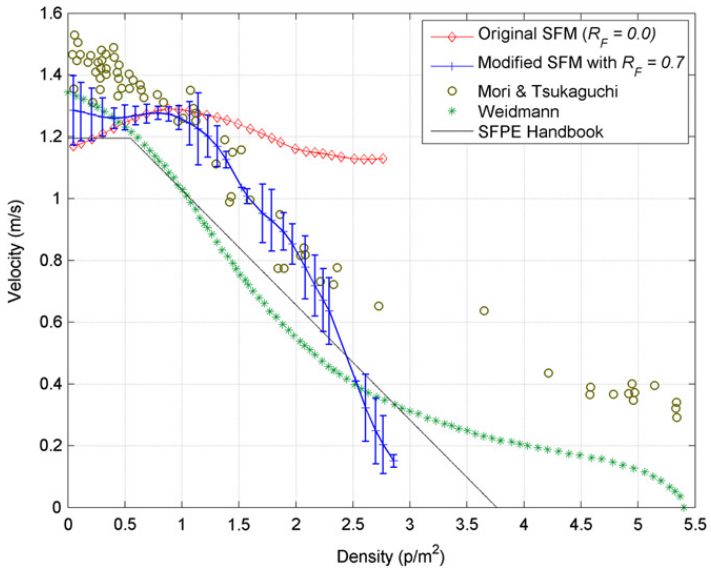

Fig. 5. Fit of the simulations performed of the modified model and comparison with the original one, experimental data given by Weidmann [10] and Mori et al. [11] and design data [16]. Error bars represent two standard deviations.

At $t = 0$, pedestrians begin to enter the racetrack. First they choose a random point, every time step, inside location "L1". Then the simulated pedestrians go to the nearest point in location "L2", "L3", and so on until they reach location "L10". After that, they try to reach a random point in location "L1" and the loop continues until the simulation ends.

Each simulation ran for 500 s. The density was calculated in the area A_R (3.5 m $\times$ 6.0 m) shown in Fig. 4, as the number of persons in A_R divided by the area A_R. Finally, the velocity corresponding to that density was calculated by averaging the instant velocities of all the pedestrian lying within area A_R.

After a transitory regime of 60 s, the system reaches a stationary state where the density fluctuates around a constant value. The positions and velocities of the particles in the system were recorded every 1 s in this stationary state.

This procedure generates a cloud of points in the fundamental diagram, that were fitted by means of a Generalized Regression Neural Networks (GRNN) [29,30]. Fig. 5 shows this fit and a comparison with the original SFM ($R_F = 0$) and with selected data reported by other authors.

The fundamental diagram produced by the modified model is similar to those reported in the literature for densities up to 2.8 p/m^2.

These reported values were taken under experimental conditions that were different to the closed-loop layout and geometry simulated here.

Also, as was mentioned in Section 1, there does not exist a unique fundamental diagram, so an exact fit of the data curves should not be expected and these curves should be considered as references.

The following comments can be made about the fundamental diagram, obtained from the modified model shown in Fig. 5:

First, if the curve obtained with $R_F = 0.7$ is compared with the one obtained from the original SFM ($R_F = 0$), it can be seen that the former decreases with higher densities and that it is near the data reported by other authors, while the curve obtained from the original SFM does not.

In the range between 0 and 1 p/m^2, the modified model shows an almost constant behavior around the mean value of the Weidmann data for that range. A possible explanation for this behavior is that, at low densities, the average interpersonal distance is large, so the condition necessary to activate the respect mechanism is seldom fulfilled, and social repulsion is low (see Eq. (2)). As a consequence, the system behaves as a non-interacting one. When the density surpasses 1 p/m^2, the respect criterion is fulfilled more frequently and, as a consequence, the mean velocity begins to decrease.

In the range between 1 and 2.3 p/m^2, the proposed method is in good agreement with the data reported by Mori and Tsukaguchi [11].

Between 2.3 and 2.8 p/m^2 the curve approaches to the Weidman [10] data again.

At 2.8 p/m^2, the boundary of validity is reached for the current model.

For densities slightly higher (around 3 p/m^2), each particle lies inside the respect area of some other particle, so the velocity of the crowd eventually becomes zero.

In general, experimental works report densities greater than 4 p/m^2 (even up to 10 p/m^2) at which the velocity becomes zero. However for design purposes (as a lower boundary), reference [16] uses the value 3.7 p/m^2, as can be seen in Fig. 5.

The stopping density around 3 p/m^2 in the simulated system is partially caused by the geometry of a closed loop. If the system were an open one, density waves would appear, avoiding the stable state in which all particles are not moving.

Another possible way to obtain greater densities before the velocity becomes zero is to use a normal distribution for the respect factor instead of taking a constant value of R_F for all particles. This would allow a few particles to have a negligible respect area, so they will continuously push other particles, generating greater velocities for high densities.

Furthermore, the maximum reachable density in the simulated system is due, also, to geometric consideration of the original SFM. The geometries of the simulated pedestrians are circular with diameters between 0.50 and 0.58 m (in our implementation).

This diameter is in accordance with the maximum body width measured at the elbows level [31].

Possible ways to obtain greater densities would be to consider: (a) a smaller diameter, corresponding to shoulder width, or even less, taking an "effective diameter" as an approximation for considering that the real human shape is not circular, (b) including elliptical-shaped particles in the calculations.

Another effect of the introduced respect mechanism is to prevent particles from entering into contact. But even if this mechanism were not present, the hardness of the particles given by the parameter k_n, would not allow much compression. In other words, the maximum density in the case of $R_F = 0$ (original SFM) would be only slightly higher than that reported here.

Beyond the limitations discussed above, which hold for both models, the improvement of the proposed modified method with respect to the original one is remarkable.

4. Conclusions

In this paper, we introduced a modification to the social force model that makes it valid for the description of the main observables of pedestrian dynamics in normal conditions.

The modification consists of a respect area parameterized by the respect factor, R_F, that provides a simple self-stopping mechanism to prevent a pedestrian from continuously pushing into other pedestrians in his/her way.

This proposed microscopic mechanism uses no direct information about any macroscopic observable such as the fundamental diagram.

Simulations of the modified model show that $R_F \approx 0.7$ matches published experimental data for normal conditions.

In this case, the specific flow rate obtained lies between the experimental range for different door widths and populations.

As for the fundamental diagram, the proposed model satisfactorily reproduces the experimental data in normal conditions for densities up to 2.8 p/m^2.

The agreement of the proposed model with the experimental data is not expected to be perfect because there are important variations among data collected by different authors under different layouts, situations, and cultures. However, if the fundamental diagram obtained by the proposed model is compared with the one obtained by the original SFM, a substantial improvement is clearly visible.

Acknowledgments

This research was supported by the agreement CONICET - URBIX TECHNOLOGIES S.A.

D.R. Parisi is a member of the 'Carrera del Investigador' CONICET Argentina.

D.R. Parisi acknowledges Luciana Bruno for useful discussion and suggestions.

The authors are very grateful to Dennis J. Linse for making useful observations, correcting the grammar and carefully editing the manuscript.

References

[1] Department of The Environment and The Welsh Office, The Building Regulations-Approved Document B - Section B1, 1992, HMSO, London, 1991, pp. 9–40.
[2] J. Fruin, Pedestrian Planning and Design, The Metropolitan Association of Urban Designers and Environmental Planners, New York, 1971.
[3] The Green Guide Guide to Safety at Sports Grounds, HSMO, London, 1991.
[4] B.D. Hankin, R.A. Wrigth, Passenger flow in subways, Oper. Res. Quart. 9 (1958) 81–88.
[5] D. Rasbash, G. Ramachandran, B. Kandola, J. Watts, M. Law, Evaluation of Fire Safety, Wiley, 2004.
[6] S.P. Hoogendoorn, W. Daamen, Pedestrian behavior at bottlenecks, Transp. Sci. 39 (2) (2005) 147–155.
[7] IMO Correspondence Group, Interim guidelines for evacuation analyses for new and existing passenger ships, Technical Report MSC/Circ.1033 International Maritime Organization (IMO), 2002.
[8] T. Kretz, A. Grünebohm, M. Schreckenberg, Experimental study of pedestrian flow through a bottleneck, J. Stat. Mech.: Theory Exp. (2006) P10014.
[9] A. Seyfried, T. Rupprecht, O. Passon, B. Steffen, W. Klingsch, M. Boltes, New insights into pedestrian flow through bottlenecks. arXiv:physics/0702004v2 [physics. soc- ph] 3 Dec 2007. Available at http://arxiv.org/abs/physics/0702004v2.
[10] U. Weidmann, Transporttechnik der Fussgänger, Transporttechnische Eigenschaften des Fussgängerverkehrs, Schriftenreihe des IVT Nr. 90, Zweite, ergänzte Auflage, Zürich, März 1993 (109 Seiten).
[11] M. Mori, H. Tsukaguchi, A new method for evaluation of level of service in pedestrian facilities, Transp. Res. A 21 A (3) (1987) 223–234.
[12] V.M. Predtetschenski, A.I. Milinski, Planning for Foot Traffic Flow in Buildings, Amerind Publishing, New Dehli, 1978.
[13] S.J. Older, Movement of pedestrians on footways in shopping streets, Traffic Eng. Control (1968).
[14] F.P.D. Navin, R.J. Wheeler, Pedestrian flow characteristics, Traffic Eng. 39 (1969) 30–36.
[15] A. Seyfried, B. Steffen, W. Klingsch, M. Boltes, The fundamental diagram of pedestrian movement revisited, J. Stat. Mech.: Theory Exp. (2005) P10002.
[16] Society of Fire Protection Engineers, SFPE Handbook of Fire Protection Engineering, National Fire Protection Association, 2002.
[17] D. Helbing, A. Johansson, H. Al-Abideen, Dynamics of crowd disasters: An empirical study, Phys. Rev. E 75 (2007) 046109.
[18] http://www.ped-net.org.
[19] A. Seyfried, B. Steffen, T. Lippert, Basics of modeling the pedestrian flow, Physica A 368 (2006) 232–238.
[20] S. Hoogendoorn, P. Bovy, W. Daamen, Microscopic pedestrian wayfinding and dynamics modeling, in: M. Schreckenberg, S. Sharma (Eds.), Pedestrian and Evacuation Dynamics, Springer, 2002, pp. 123–155.
[21] D. Helbing, P. Molnár, Social force model for pedestrian dynamics, Phys. Rev. E 51 (1995) 4282.
[22] D. Helbing, I. Farkas, T. Vicsek, Simulating dynamical features of escape panic, Nature 407 (2000) 487.
[23] D. Helbing, I. Farkas, T. Vicsek, Freezing by heating in a driven mesoscopic system, Phys. Rev. Lett. 84 (2000) 1240.
[24] D. Helbing, Traffic and related self-driven many-particle systems, Rev. Modern Phys. 73 (2001) 1067.
[25] D. Helbing, Similarities between granular and traffic flow, in: H.J. Herrmann, et al. (Eds.), Physics of Dry Granular Media, Kluwer Academic Publishers, 1998, pp. 547–552.
[26] D. Helbing, I. Farkas, P. Molnar, T. Vicsek, in: M. Schreckenberg, S.D. Sharma (Eds.), Pedestrian and Evacuation Dynamics, Springer, 2001, p. 21.
[27] T.I. Lakoba, D.J. Kaup, N.M. Finkelstein, Modifications of the Helbing–Molnár–Farkas–Vicsek social force model for pedestrian evolution, Simulation 81 (2005) 339–352.
[28] J.M. Haile, Molecular Dynamics Simulation, Wiley-Interscience Publication, 1997.
[29] D. Patterson, Artificial Neural Networks, Prentice Hall, Singapore, 1996.
[30] C. Bishop, Neural Networks for Pattern Recognition, University Press, Oxford, 1995.
[31] Preliminary human factors guidelines for traffic management centers, Publication Number: FHWA-JPO-99-042, U.S. Department of Transportation - Federal Highway Administration, July 1999. Available at: http://ergotmc.gtri.gatech.edu/dgt/.